DOI: 10.1002/asia.200800388

Bridging M−Cl Bonds with Ambiphilic Phosphine–Borane Ligands

Sébastien Bontemps,[a] Ghenwa Bouhadir,[a] David C. Apperley,[b] Philip W. Dyer,[b] Karinne Miqueu,*[c] and Didier Bourissou*[a]

Abstract: A combined experimental/theoretical study provides insight into the bridging coordination of M−Cl bonds with the ambiphilic phosphine–borane ligands iPr$_2$P-o(C$_6$H$_4$)-BR$_2$ (PBCy$_2$: R = Cy; PBMes$_2$: R = Mes). Reaction of [PdCl(allyl)(PBCy$_2$)] (**3**) with HCl affords the related dinuclear complex [PdCl(μ-Cl)(PBCy$_2$)]$_2$ (**5**). Subsequent cleavage of the chloride bridge by PPh$_3$ leads to the heteroleptic mononuclear complex *trans*-[PdCl$_2$(PPh$_3$)(PBCy$_2$)] (**6**). The solid-state structures of complexes **5** and **6** substantiate the propensity of the PBCy$_2$ ligand to bridge Pd-Cl bonds via P→Pd−Cl→B interactions. DFT calculations carried out on both the model mononuclear complexes **3*** and **6*** reveal that in each system the energy of the linkage isomer with a Cl→B interaction is very similar to that without. A comparison of the solution and solid-state ^{11}B NMR spectroscopic data for complexes **3** and **6** suggests the possible interconversion of the bridging and B-pendant forms in solution. Bridging coordination of the PBCy$_2$ ligand across a Rh−Cl bond is observed in the solid-state structure of the related complex [RhCl(nbd)(PBCy$_2$)] (**7**). Replacement of the Cy groups at boron by Mes substituents illustrates the role of steric factors on the participation of the Lewis acid upon coordination, no Cl→B interaction being observed in the complex [PdCl(allyl)(PBMes$_2$)] (**8**).

Keywords: ambiphilic ligands · boranes · density functional calculations · NMR spectroscopy · X-ray diffraction

Introduction

Over the last few years there has been an ever-growing interest in the use of ambiphilic compounds as ligands for transition metals.[1–7] By varying the nature of the donor (phosphine, pyridine) and acceptor (borane, alane) sites, different coordination modes of such ligands have been established (Figure 1). In particular, the presence of donor buttresses has been exploited to support M→borane interactions (coordination mode **I**),[8–10] thereby affording a better understanding of the properties of the σ-acceptor bonding component. The introduction of a pendant Lewis acid (coordination mode **II**)[11] in the secondary coordination sphere, potentially susceptible to interaction with a substrate or a co-ligand, has also been illustrated. Furthermore, a small number of complexes have been prepared that substantiate the ability of ambiphilic ligands to bridge M−X bonds (coordination mode **III**).[10b,c,g,12] Such a bridging coordination mode represents a preliminary stage in the intramolecular activation of M−X bonds,[13] which can ultimately form zwitterionic complexes (coordination mode **IV**), as the result of X abstraction from the metal by the Lewis acid.[14]

Herein we report a combined experimental/theoretical study focused on the bridging coordination of the ambiphilic

[a] Dr. S. Bontemps, Dr. G. Bouhadir, Dr. D. Bourissou
Laboratoire Hétérochimie Fondamentale et Appliquée du CNRS (UMR 5069)
Equipe Ligands Bifonctionnels et Polymères Biodégradables
Université Paul Sabatier
118 route de Narbonne, 31062 Toulouse Cedex 09 (France)
Fax: (+33) 5-61 55 82 04
E-mail: dbouriss@chimie.ups-tlse.fr

[b] Dr. D. C. Apperley, Dr. P. W. Dyer
Department of Chemistry
Durham University
South Road, Durham, DH1 3LE (United Kingdom)

[c] Dr. K. Miqueu
Institut Pluridisciplinaire de Recherche sur l'Environnement et les Matériaux (UMR 5254)
Equipe Chimie-Physique
Université de Pau et des Pays de l'Adour
Hélioparc, 2 Avenue du Président Angot, 64053 Pau cedex 09 (France)
Fax: (+33) 5-59 40 78 62
E-mail: Karinne.Miqueu@univ-pau.fr

Supporting information for this article is available on the WWW under http://dx.doi.org/10.1002/asia.200800388.

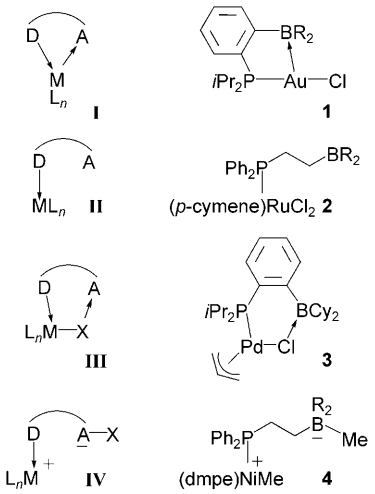

Figure 1. Different coordination modes of ambiphilic ligands with representative examples utilising phosphine–boranes ($BR_2 = BCy_2$ or 9-BBN).

ligand *i*Pr_2P-*o*(C_6H_4)-BCy_2 (referred to as $PBCy_2$) across Pd–Cl and Rh–Cl bonds. The solid-state structures of [PdCl(μ-Cl)($PBCy_2$)]$_2$ (**5**), *trans*-[$PdCl_2$(PPh_3)($PBCy_2$)] (**6**), and [RhCl(nbd)($PBCy_2$)] (**7**) illustrate the propensity of $PBCy_2$ to engage in bridging P→M–Cl→B interactions. The coordination modes with and without Cl→B interaction are predicted computationally to be very close in energy, with ^{11}B NMR data supporting the possible interconversion of the two forms in solution. Additionally, the influence of steric factors on the participation of the Lewis acid within a metal's coordination sphere has been investigated using the more sterically demanding ligand *i*Pr_2P-*o*(C_6H_4)-$BMes_2$ (referred to as $PBMes_2$).

Results and Discussion

Synthesis andCharacterization of the Palladium Complexes [PdCl(μ-Cl)($PBCy_2$)]$_2$ (5) and *trans*-[$PdCl_2$(PPh_3)($PBCy_2$)] (6)

Complex **3**, readily prepared from $PBCy_2$ and [Pd(μ-Cl)(allyl)]$_2$,[10b] reacted cleanly with HCl at room temperature in CH_2Cl_2. After 24 h, the reaction was complete and the dinuclear complex [PdCl(μ-Cl)($PBCy_2$)]$_2$ (**5**) was subsequently isolated as a white powder in 59% yield (Scheme 1). The loss of the allyl ligand is readily apparent from the ^{1}H NMR spectrum of **5**, with the ^{31}P NMR signal observed at $\delta =$ 60.3 ppm being indicative of the retention of the $PBCy_2$

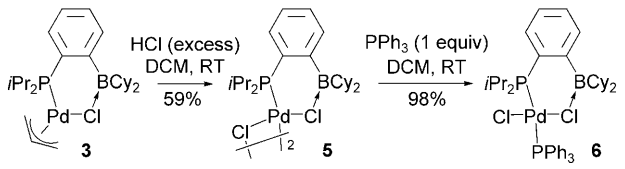

Scheme 1. Synthesis of the palladium complexes [PdCl(μ-Cl)($PBCy_2$)]$_2$ (**5**) and *trans*-[$PdCl_2$(PPh_3)($PBCy_2$)] (**6**).

ligand in the coordination sphere of palladium. However, no ^{11}B NMR signal could be detected from a solution of **5**.

To gain greater insight into the precise structure of complex **5**, crystals suitable for study by X-ray diffraction (XRD) were grown from a CH_2Cl_2 solution at −40 °C. The resulting molecular structure is shown in Figure 2, with selected geometric data collected in Table 1. Complex **5** adopts a centrosymmetric and planar[15] chloro-bridged structure in the solid state. The palladium center is ligated by one phosphorus and three chlorine atoms, which are organized in a perfectly planar arrangement ($\Sigma Pd_\alpha = 360°$). The chloride ligand not involved in the [Pd(μ-Cl)]$_2$ bridge interacts with the boron atom so that the $PBCy_2$ ligand retains its ambiphilic bridging coordination toward the Pd–Cl bond. Notably, the Cl–B bond distance determined for **5** (2.334(7) Å) is substantially greater than that of **3** (2.165(2) Å).[10b] Along with the less pyramidalized environment around boron ($\Sigma B_\alpha = 353.7°$ in **5** vs. 349.1° in **3**), these

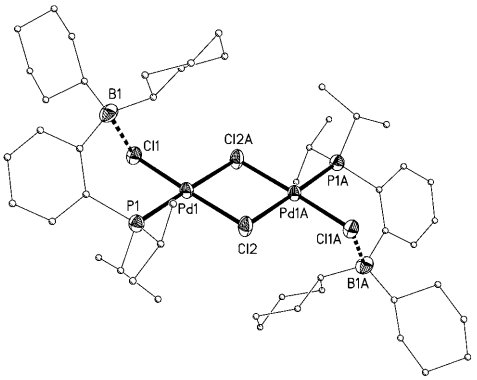

Figure 2. Molecular structure of the palladium complex [PdCl(μ-Cl)($PBCy_2$)]$_2$ (**5**) with hydrogen atoms and solvate molecules omitted.

Table 1. Geometric data (bond lengths and angles in Å and °, respectively) determined experimentally for complexes **3**,**5**–**8** and computed at the B3PW91/SDD(Pd,Rh),6–31G**(other atoms) level of theory for model complexes **3***,**6***–**8***.

			P–M	M–Cl	Cl···B	ΣB_α	ΔG_{298}[b]
3	X-ray	bridging	2.296(1)	2.352(1)	2.165(2)	349.1	
3*	DFT	bridging	2.303	2.366	2.123	340.9	0
3*	DFT	B-pendant	2.323	2.370	4.568	358.2	−4.9
5	X-ray	bridging	2.233(2)	2.263(2)[a]	2.334(7)	353.7	
				2.324(2)			
				2.433(2)			
6	X-ray	bridging	2.348(1)	2.280(1)[a]	2.109(4)	343.5	
				2.304(2)			
6*	DFT	bridging	2.334	2.324	2.155	344.6	0
				2.335			
6*	DFT	B-pendant	2.361	2.334	4.339	358.4	−3.5
				2.342			
7	X-ray	bridging	2.298(1)	2.344(1)	2.117(2)	342.6	
7*	DFT	bridging	2.037	2.385	2.144	342.9	0
7*	DFT	B-pendant	2.312	2.359	3.897	358.4	3.0
8	X-ray	B-pendant	2.334(2)	2.370(1)	4.381(5)	358.9	
8*	DFT	B-pendant	2.327	2.362	5.306	359.3	

[a] Pd–Cl bond engaged in Cl→B interaction.[b] Calculated at 298.15 K.

observations suggest some weakening of the Cl→B interaction following loss of the allyl ligand and subsequent Pd–Cl bridge formation.

Complex **5** was then reacted with PPh_3, a representative Lewis base capable of cleaving the $[Pd(\mu\text{-}Cl)]_2$ bridge and/or the Cl→B interaction.[16] The reaction proceeds readily at room temperature in CH_2Cl_2 and affords selectively the heteroleptic mononuclear complex **6**, isolated in 93% yield as a pale yellow solid. The two doublets observed in the ^{31}P NMR spectrum of **6** ($\delta = 34.8$ and 20.0 ppm, $^2J(P,P) = 497.2$ Hz) are diagnostic of the *trans* coordination of the two phosphines to the Pd center.[17] As for its precursor **5**, no ^{11}B NMR resonance signal could be detected in solution for **6**. This prompted us to characterize further the mononuclear complex **6** by solid-state NMR spectroscopy. The ^{31}P NMR spectrum (two doublets at $\delta = 34.6$ and 23.6 ppm, $^2J(P,P) = 488$ Hz) mirrors that obtained in solution, whereas the ^{11}B NMR spectrum presents a distinct signal at $\delta = 22$ ppm. The latter value is identical to that found for the bridging N→Ru–Cl→B coordination of the $[RuCl_2(cymene)]$ fragment by the pyridine–borane ligand (2-picolyl)BCy_2 (δ $^{11}B = 22$ ppm in CD_2Cl_2 solution),[12d] suggesting the retention of the Cl→B interaction in **6**.

To confirm this bonding situation, crystals of **6** were grown from a CH_2Cl_2/pentane mixture at −40 °C, and an XRD analysis was carried out (Figure 3). The palladium

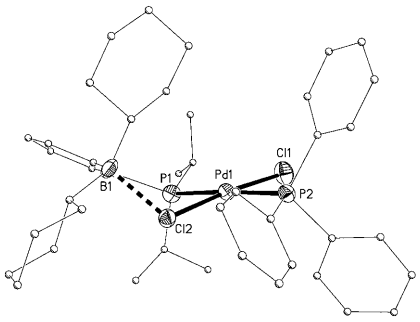

Figure 3. Molecular structure of the palladium complex *trans*-$[PdCl_2(PPh_3)(PBCy_2)]$ (**6**) with hydrogen atoms and solvate molecules omitted.

center adopts a near-perfect *trans* square-planar geometry ($\Sigma Pd_\alpha = 359.8°$, Cl-Pd-Cl = 175.17(4)°, P-Pd-P = 177.43(4)°). One of the two chloride ligands interacts with the boron atom (B–Cl = 2.109(4) Å, $\Sigma B_\alpha = 343.5°$). The replacement of the chloride-bridge by the more basic PPh_3 ligand on going from complex **5** to **6** results in a substantial strengthening of the Cl→B interaction. Notably, complexation of the Lewis acid moiety does not noticeably affect the Pd–Cl bond lengths in **6** (2.280(1) Å for the Pd–Cl bond engaged in Cl→B interaction vs. 2.304(1) Å for the other Pd–Cl bond). This situation is reminiscent of those encountered in the $[TpOsCl_2(N(Ph)BPh_2)]$ ($\Delta d_{OsCl} < 0.07$ Å)[12c] and [*p*-(cymene)$RuCl_2$(picoBCy_2)] ($\Delta d_{RuCl} < 0.05$ Å)[12d] complexes. In fact, to date, substantial elongation of an M-Cl bond upon coordination to a Lewis acid has only been observed with very electrophilic moieties such as in [Cp{Cp(B-$(C_6F_5)_2$)$TiCl_2$] ($\Delta d_{TiCl} = 0.14$ Å).[12b]

At this point, the solution-state ^{11}B NMR spectroscopic data for complex **3** deserve some comment. Indeed, the resonance signal observed for **3** in $CDCl_3$ ($\delta = 47$ ppm) is significantly shielded compared to that of the free ligand $PBCy_2$ ($\delta = 76$ ppm),[10b] but appears at noticeably higher frequency than that of the related complex **6** ($\delta = 22$ ppm in the solid-state). By analogy with the situation encountered for di- and tri-phosphine–borane ligands,[18] it was envisaged that the intermediate ^{11}B NMR chemical shift of **3** could result from an equilibrium between the bridging and B-pendant forms, namely coordination modes **III** and **II**, respectively. To further explore this possibility,[19] DFT calculations were carried out.

DFT Calculations on the Palladium Complexes [PdCl(allyl)(PBCy$_2$)] (3*) and *trans*-[PdCl$_2$(PMe$_3$)(PBCy$_2$)] (6*)

Calculations were performed at the B3PW91/SDD(Pd),6-31G**(other atoms) level of theory that has already proved appropriate for transition-metal complexes featuring ambiphilic ligands.[10d–f] The model mononuclear complexes **3*** and **6*** retain the Cy substituents at the boron atom, but feature Me instead of *i*Pr/Ph groups at the phosphorus atoms. For each complex, an energy minimum associated with the linkage isomer with P→Pd–Cl→B bridging coordination was located on the potential energy surface (PES). The optimized geometries (Figure 4, Table 1) are in very good agreement with those observed crystallographically (key bond distances are reproduced with an error of less than ±0.05 Å), indicating the reliability of the computational method used. Natural bond orbital (NBO) analyses further substantiated the presence of significant Cl→B interactions. Indeed, a

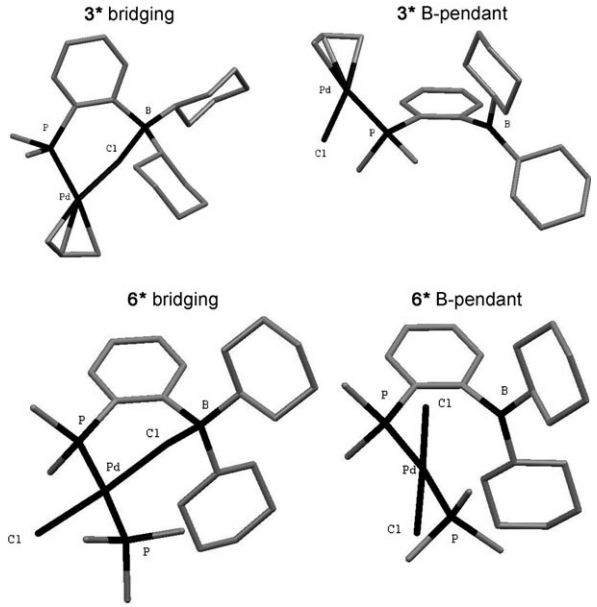

Figure 4. Optimized structures of the bridging and B-pendant forms of **3*** and **6***.

strongly polarised Cl–B bond (20.1% B/79.9% Cl) was found at the first-order in **3***, and a strong Cl→B interaction (ca. 108 kcal mol^{-1}) was found at the second-order donor–acceptor perturbation level in **6***. Following rotation around the P–Pd bond, another minimum corresponding to the B-pendant coordination mode **II** of the ambiphilic ligand was found for both complexes. The long Cl···B and Pd···B distances (>3.7 Å), and the replanarization of the boron environments (ΣB_α ca. 360°) rule out any significant Cl→B and Pd→B interaction. A comparison of the NPA atomic charges (Table 2) for the bridging and B-pendant forms indicates

Table 2. Atomic charges, as derived from natural population analyses (NPA), computed for model complexes **3***, **6***, and **7***.

		q(P)	q(M)	q(Cl)	q(B)
3*	bridging	1.07	0.37	−0.26	0.65
3*	B-pendant	1.04	0.38	−0.61	1.02
6*	bridging	1.10	0.28	−0.24, −0.53	0.69
6*	B-pendant	1.08	0.32	−0.54, −0.55	1.02
7*	bridging	1.16	0.09	−0.24	0.67
7*	B-pendant	1.14	0.09	−0.54	1.02

that the Cl→B interaction is associated with a formal transfer of about 0.4 of an electron from Cl to B for **3*** and 0.3 of an electron for **6***. As a consequence, the Pd–Cl→B bridging creates a charge asymmetry between the two chloride ligands of **6*** (the atomic charge of the chloride engaged in the interaction with the borane is −0.24 vs. −0.53 for the other chloride). Notably, the net charge at the metal center remains unchanged upon coordination of the chloride ligand to the Lewis acid.

For both complexes **3*** and **6***, the bridging and B-pendant forms lie very close in energy (ΔG_{298} = 4.9 and 3.5 kcal mol^{-1} for **3*** and **6***, respectively), supporting the hypothesis of an equilibrium between these two coordination modes in solution. This has been further corroborated by computing the ^{11}B NMR chemical shifts of both forms of the model complex **3*** using the GIAO method. The value predicted for the bridged structure (δ = 17 ppm) agrees nicely with the chemical shift determined experimentally in the solid state for **6** (δ = 22 ppm), whereas that estimated for the B-pendant form (δ = 79 ppm) is comparable to that measured for the free ligand $PBCy_2$ (δ = 76 ppm). The value obtained in $CDCl_3$ solution for **3** (δ = 47 ppm) is thus intermediate between those computed for the bridging and B-pendant forms, in line with the coexistence of the two coordination modes in solution.

Synthesis, Characterization, and DFT Calculations of the Rhodium Complex [RhCl(nbd)($PBCy_2$)] (7)

To further probe the propensity of the phosphine–borane ligand $PBCy_2$ to bridge M-Cl bonds, it was reacted with [Rh(μ-Cl)(nbd)]$_2$ (nbd = 2,5-norbornadiene) in CH_2Cl_2 (Scheme 2). The resulting rhodium complex [RhCl(nbd)($PBCy_2$)] (**7**) was isolated in 62% yield as an orange solid.

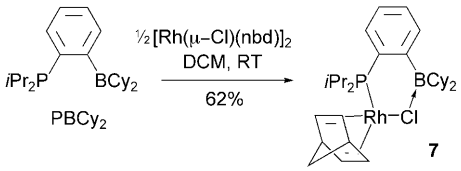

Scheme 2. Synthesis of the rhodium complex [RhCl(nbd)($PBCy_2$)] (**7**).

The coordination of the phosphorus atom to the rhodium center was indicated unambiguously by the ^{31}P NMR spectrum (doublet at δ = 32.5 ppm, ^1J(P,Rh) = 160 Hz), whereas retention of the norbornadiene co-ligand was apparent from the ^{1}H and ^{13}C NMR spectra. As for the Pd complexes **5** and **6**, no ^{11}B NMR signal could be detected in solution for **7**, and thus solid-state NMR spectroscopy was carried out to shed more light onto the coordination mode of the $PBCy_2$ ligand. The ^{31}P NMR spectrum (doublet at δ = 32.5 ppm, ^1J(P,Rh) = 160 ± 4 Hz) agreed well with that measured in solution, whereas the signal observed at δ = 26 ppm in the ^{11}B NMR spectrum mirrored that found for the mononuclear complex **6**, consistent with P→Rh–Cl→B bridging coordination in **7**.

To confirm further this bonding situation, single crystals of **7** suitable for XRD analysis were grown from a saturated CH_2Cl_2 solution at −40 °C (Figure 5). The complex indeed

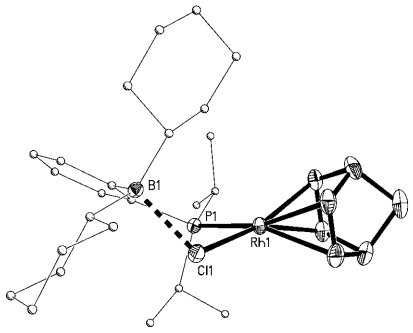

Figure 5. Molecular structure of the rhodium complex [RhCl(nbd)($PBCy_2$)] (**7**) with hydrogen atoms omitted.

adopts a six-membered ring structure as the result of the bridging coordination of the Rh-Cl unit by the ambiphilic ligand. The strong Cl→B interaction is supported by the short Cl–B distance (2.117(2) Å) and the noticeable pyramidalization of the boron center (ΣB_α = 342.6°).

DFT calculations were carried out at the B3PW91/SDD(Rh),6-31G**(other atoms) level of theory on the model complex **7*** featuring Me instead of *i*Pr substituents at the phosphorus atom. Two minima were found on the PES (Figure 6). The first minimum agreed well with the bridged geometry observed in the XRD analysis, whereas the second, featuring long B···Cl and Rh···B distances (> 3.7 Å), corresponds to the B-pendant form. NBO analyses revealed the presence of a strong Cl→B interaction in the bridged structure at the second-order perturbation level (ca.

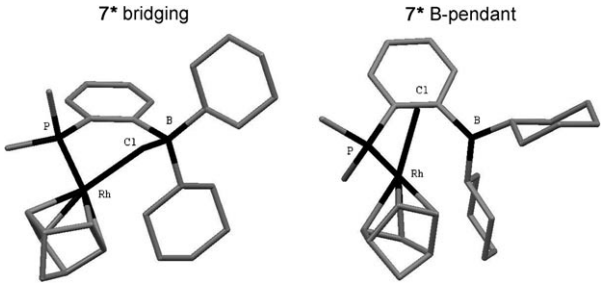

Figure 6. Optimized structures of the bridging and B-pendant forms of **7***.

215 kcal mol^{-1}), accompanied by a formal transfer of 0.3 of an electron from the chloride to the boron atom. In contrast, no modification of the atomic charge at the rhodium center of **7*** was observed (as deduced from a comparison of the NPA charges computed for the two minima). For the model complex **7***, the B-pendant form is only 3.0 kcal mol^{-1} higher in energy than its bridged counterpart, suggesting once again a possible equilibrium between both coordination modes in solution. Furthermore, very good agreement was found between the ^{11}B NMR chemical shift computed for the bridging form of **7*** ($\delta = 25$ ppm) and that determined experimentally in the solid-state for **7** ($\delta = 26$ ppm), while a chemical shift at much higher frequency was predicted for the B-pendant structure of **7*** ($\delta = 75$ ppm).

Synthesis, Characterization, and DFT Calculations of the Palladium Complex [PdCl(allyl)(PBMes$_2$)] (8)

Finally, the role of steric factors on the participation of the Lewis acid moiety was assessed through study of the related PBMes$_2$ ligand[6,7] featuring mesityl instead of cyclohexyl groups at the boron atom. No reaction occurred with [Rh(μ-Cl)(nbd)]$_2$, but [Pd(μ-Cl)(allyl)]$_2$ was readily cleaved by PBMes$_2$ in CH_2Cl_2 at room temperature to give the corresponding mononuclear complex **8**, isolated in 42% yield as a yellow solid (Scheme 3). The coordination of the phosphorus atom was unambiguously established by ^{31}P NMR spectroscopy ($\delta = 50.8$ ppm), whereas the ^{11}B NMR chemical shift determined for the complex ($\delta = 73$ ppm in $CDCl_3$) is very similar to that of the free ligand ($\delta = 76$ ppm), suggesting negligible, if any, participation of the borane in the coordination.

Single crystals of **8** were grown from a mixed Et_2O/THF solution at −40 °C (Figure 7). The XRD analysis confirmed that the ambiphilic ligand adopts a B-pendant arrangement (coordination mode **III**). The phosphorus atom is coordinated to the metal center, but the Cl···B (4.381(5) Å) and

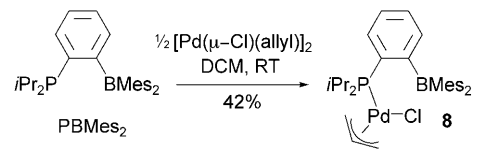

Scheme 3. Synthesis of the palladium complex [PdCl(allyl)(PBMes$_2$)] (**8**).

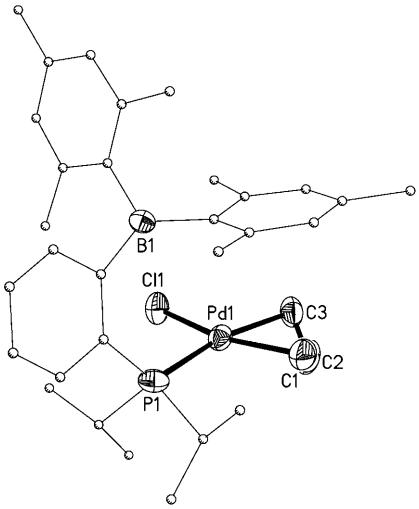

Figure 7. Molecular structure of the palladium complex [PdCl(allyl)-(PBMes$_2$)] (**8**) with hydrogen atoms omitted.

Pd···B (3.850(5) Å) distances are far too long for any substantial bonding interaction between the borane and the metal fragment. Moreover, the geometry at boron deviates only marginally from planarity ($\Sigma B_\alpha = 358.9°$). Notably, one of the mesityl rings is orientated near-parallel to the metal square plane, but the palladium–carbon distances are too long (>3.5 Å) to be associated with any π-type interaction, as has been observed in complexes derived from biarylphosphines.[20]

To gain more insight into the lack of any Cl→B interaction in **8**, DFT calculations were performed on the model complex **8*** featuring Me instead of *i*Pr groups at the phosphorus atom. An energy minimum associated with the B-pendant form was found on the PES (Table 1). The ^{11}B NMR chemical shift computed for the optimized structure ($\delta = 68$ ppm) is in good agreement with that measured experimentally in solution ($\delta = 73$ ppm). Despite extensive effort and regardless of the initial geometry, no minimum corresponding to a bridging form featuring a Cl→B interaction could be located in this model system. The greater steric hindrance of the mesityl groups is likely to prevent participation of the Lewis acid.[21]

Conclusions

These results provide insight into the bridging coordination of M−Cl bonds with phosphine–borane ligands. The solid-state structures of complexes **3**, **5**, and **6** illustrate the propensity of the ambiphilic ligand PBCy$_2$ to bridge Pd−Cl bonds, and the ability of Cl→B interactions to persist in the presence of HCl as well as PPh$_3$. DFT calculations substantiate the presence of strong Cl→B interactions associated with a formal transfer of about 0.3 to 0.4 of an electron. Furthermore, the bridging and B-pendant coordination modes are predicted to be very close in energy, and their possible coexistence in solution is suggested by the comparison of

the solution and solid-state ^{11}B NMR spectroscopic data for complexes **3** and **6**.[22] The related rhodium complex **7** exhibits similar bridging coordination of the $PBCy_2$ ligand across the Rh–Cl bond in the solid-state. Finally, the B-pendant arrangement adopted by the palladium complex **8** deriving from $PBMes_2$ illustrates the role of steric factors in the coordination, or not, of the Lewis acid.

Arising from their ability to adopt various coordination modes, which can even interconvert, phosphine–boranes are particularly versatile ligands. Further investigations in this area will aim to provide evidence for the possible coexistence of the zwitterionic form **IV** with another coordination mode. Together, these studies will provide a precise understanding of the coordination properties of ambiphilic ligands, something that will facilitate the incorporation of these metal scaffolds into catalytic systems in the future.

Experimental Section

General

All reactions and manipulations were carried out under an atmosphere of dry argon using standard Schlenk techniques. THF and diethyl ether were dried over sodium/benzophenone, CH_2Cl_2 was dried over P_2O_5, and pentane was dried over CaH_2 and distilled prior to use. ^1H, ^{13}C, ^{11}B, ^{31}P, and ^{103}Rh NMR spectra were recorded on Brucker Avance 300 or AMX 500 spectrometers. Chemical shifts are expressed with a positive sign, in parts per million, relative to residual ^1H and ^{13}C solvent signals, external $BF_3{\cdot}OEt_2$, 85% H_3PO_4, and $\Xi = 3.186447$ MHz, respectively. Solid-state NMR spectra were recorded on a Varian VNMRS 400 spectrometer (referencing is as for solution). Whatever the conditions of acquisition, no ^{11}B NMR resonance signal could be detected in solution for complexes **5**, **6**, and **7**. The solid-state boron isotropic chemical shifts were determined from a numerical simulation of the bandshape using the Varian STARS software. Unless otherwise stated, NMR spectra were recorded at 20 °C. Mass spectra were recorded on a Hewlett Packard 5989 A. The $PBCy_2$ and $PBMes_2$ ligands and the [PdCl(allyl)($PBCy_2$)] complex **3** were prepared following published procedures.[6,10b]

Syntheses

[PdCl(μ-Cl)($PBCy_2$)]$_2$ (**5**)*:* To a suspension of complex **3** (2.10 g, 3.80 mmol) in CH_2Cl_2 (10 mL) at room temperature was added an excess of HCl in Et_2O solution (18.9 mL, 2 M, 37.8 mmol). After subsequent stirring for 24 h, the solution was filtered off. The volatiles were removed and the solid was washed with CH_2Cl_2 (2*10 mL). Complex **4** was obtained as a white powder (1.23 g, 59% yield). Colorless crystals suitable for X-ray crystallography were obtained from a CH_2Cl_2 solution at −40 °C; m.p. 157–159 °C; $^{31}P\{^1H\}$ NMR (202.5 MHz, $CDCl_3$, −30 °C): $\delta =$ 60.3; $^{13}C\{^1H\}$ NMR (125.8 MHz, $CDCl_3$, −30 °C): $\delta = 159.0$ (d, $^2J(P,C) =$ 14.4 Hz; BC_{ipso}), 132.9 (d, $J(P,C) = 14.4$ Hz; CH_{arom}), 130.3 (d, $J(P,C) =$ 6.6 Hz; CH_{arom}), 129.2 (s; CH_{arom}), 124.4 (d, $J(P,C) = 10.5$ Hz; CH_{arom}), 123.2 (d, $^1J(P,C) = 56.3$ Hz; PC_{ipso}), 30.6 (br; Cy), 30.1 (s; Cy), 29.3 (s; Cy), 28.3 (s; Cy), 27.6 (s; Cy), 27.0 (d, $^1J(P,C) = 18.3$ Hz; CH *i*Pr), 19.2 (s; Cy), 18.6 ppm (br; CH_3 *i*Pr); ^1H NMR (500.3 MHz, $CDCl_3$, −30 °C): $\delta =$ 7.51 (dd, $^3J(H,H) = 7.6$ Hz, $^4J(P,H) = 3.9$ Hz, 1H; H_{arom}), 7.40 (pseudo-t, $^3J(H,H) = 7.6$ Hz, 1H; H_{arom}), 7.35 (pseudo-t, $^3J(H,H) = {}^3J(P,H) = 7.6$ Hz, 1H; H_{arom}), 7.19 (pseudo-t, $^3J(H,H) = 7.6$ Hz, 1H; H_{arom}), 2.59 (br, 2H; CH *i*Pr), 2.22 (m, 2H; Cy), 1.81 (m, 2H; Cy), 1.71 (m, 2H; Cy), 1.61 (m, 2H; Cy), 1.30–1.48 (m, 10H; Cy), 1.24 (dd, $^3J(H,H) = 6.7$ Hz, $^3J(P,H) =$ 15.4 Hz, 12H; CH_3 *i*Pr), 1.17 (m, 2H; Cy), 1.12 ppm (m, 2H; Cy).

trans-[$PdCl_2(PPh_3)(PBCy_2)$] (**6**): To a suspension of complex **4** (145 mg, 0.13 mmol) in CH_2Cl_2 (5 mL) at room temperature was added PPh_3 (65 mg, 0.25 mmol, 3 mL) in CH_2Cl_2 solution (3 mL). After 15 min, the volatiles were removed and the solid was extracted with Et_2O. Colorless crystals of **6** (103 mg, 98%) suitable for X-ray crystallography were obtained from a CH_2Cl_2/pentane solution at −40 °C; m.p. 171 °C; $^{31}P\{^1H\}$ NMR (202.5 MHz, $CDCl_3$): $\delta = 34.8$ (d, $^2J(P,P) = 497.2$ Hz, P*i*Pr_2), 20.0 (d, $^2J(P,P) = 497.2$ Hz, PPh_3); $^{31}P\{^1H\}$ NMR (161.9 MHz, solid state): $\delta = 34.6$ (d, $^2J(P,P) = 488$ Hz, P*i*Pr_2), 23.6 ppm (d, $^2J(P,P) = 488$ Hz, PPh_3); ^{11}B NMR (128.3 MHz, solid state): $\delta = 22$ ppm; $^{13}C\{^1H\}$ NMR (125.8 MHz, $CDCl_3$): $\delta = 161.0$ (d, $^2J(P,C) = 18.6$ Hz; BC_{ipso}), 135.0 (d, $J(P,C) = 10.6$ Hz; CH_{arom} Ph_3P), 133.0 (d, $J(P,C) = 12.7$ Hz; CH_{arom}), 131.0 (dd, $J(P,C) = 6.7$ Hz, $J(P,C) = 4.4$ Hz; CH_{arom} Ph_3P), 130.6 (d, $J(P,C) =$ 2.0 Hz; CH_{arom} Ph_3P), 129.0 (dd, $^1J(P,C) = 42.5$ Hz, $^3J(P,C) = 3.3$ Hz; PC_{ipso} Ph_3P), 128.3 (d, $J(P,C) = 10.4$ Hz; CH_{arom} Ph_3P), 128.2 (br; CH_{arom} Ph_3P), 125.8 (dd, $^1J(P,C) = 41.5$ Hz, $^3J(P,C) = 4.6$ Hz; PC_{ipso}), 123.5 (d $J(P,C) =$ 5.7 Hz; CH_{arom}), 35.0 (s; Cy), 31.1 (s; Cy), 30.4 (s; Cy), 29.1 (s; Cy), 28.7 (s; Cy), 27.7 (s; Cy), 26.0 (d, $^1J(P,C) = 22.0$ Hz; CH *i*Pr), 19.8 (d, $^2J(P,C) =$ 3.7 Hz; CH_3 *i*Pr), 19.2 ppm (br; CH_3 *i*Pr); ^1H NMR (500.3 MHz, $CDCl_3$): $\delta = 7.71$ (m, 6H; H_{arom}), 7.53 (m, 1H; H_{arom}), 7.51–7.46 (m, 9H; H_{arom}), 7.32 (m, 2H; H_{arom}), 7.15 (m, 1H; H_{arom}), 3.09 (septd, $^3J(H,H) = 6.9$ Hz, $^2J(P,H) = 4.3$ Hz, 2H; CH *i*Pr), 2.12 (m, 2H; Cy), 1.69–1.56 (m, 6H; Cy), 1.45 (m, 2H; Cy), 1.35 (dd, $^3J(H,H) = 6.9$ Hz, $^3J(P,H) = 17.5$ Hz, 6H; CH_3 *i*Pr), 1.30 (dd. $^3J(H,H) = 6.9$ Hz, $^3J(P,H) = 13.8$ Hz, 6H; CH_3 *i*Pr), 1.10 (m, 6H; Cy), 0.97 (m, 2H; Cy), 0.87 ppm (m, 4H; Cy).

[RhCl(nbd)($PBCy_2$)] (**7**)*:* To a solution of ligand $PBCy_2$ (258 mg, 0.70 mmol) in CH_2Cl_2 (7 mL) at −78 °C was added a solution of [Rh(μ-Cl)(nbd)]$_2$ (160 mg, 0.35 mmol) in CH_2Cl_2 (7 mL). The solution was warm to room temperature within 1 h. Orange crystals of **7** (260 mg, 62%) suitable for X-ray crystallography were obtained from a saturated solution of CH_2Cl_2 at −40 °C; m.p. 172–174 °C. $^{31}P\{^1H\}$ NMR (202.5 MHz, $CDCl_3$, 0 °C): $\delta = 32.5$ ppm (d, $^1J(Rh,P) = 160.0$ Hz); $^{31}P\{^1H\}$ NMR (161.9 MHz, solid state): $\delta = 32.5$ ppm (d, $^1J(Rh,P) = 160.0$ Hz); ^{11}B NMR (128.3 MHz, solid state): $\delta = 26$ ppm; ^{103}Rh NMR (202.5 MHz, $CDCl_3$, 0 °C): $\delta = -7720$; $^{13}C\{^1H\}$ NMR (125.8 MHz, $CDCl_3$, 0 °C): $\delta = 160.1$ (d, $^2J(P,C) = 18.5$ Hz; BC_{ipso}), 132.2 (d, $J(P,C) = 12.9$ Hz; CH_{arom}), 130.9 (s; CH_{arom}), 129.7 (d, $^1J(P,C) = 37.3$ Hz; PC_{ipso}), 127.7 (d, $J(P,C) = 2.5$ Hz; CH_{arom}), 123.9 (d, $J(P,C) = 6.3$ Hz; CH_{arom}), 81.4 (dd, $J(Rh,C) = 5.5$ Hz, $J(P,C) = 10.7$ Hz; CH_{alkene} nbd), 64.0 (d, $J(Rh,C) = 4.9$ Hz; CH_2 nbd), 52.4 (d, $J(Rh,C) = 12.6$ Hz; CH_{alkene} nbd), 50.9 (d, $J(P,C) = 1.3$ Hz; CH nbd), 36.4 (s; Cy), 32.0 (s; Cy), 30.6 (s; Cy), 29.2 (s; Cy), 29.1 (s; Cy), 27.9 (s; Cy), 26.5 (d, $^1J(P,C) = 21.6$ Hz; CH *i*Pr), 20.3 (d, $^2J(P,C) = 3.8$ Hz; CH_3 *i*Pr), 18.9 ppm (s; CH_3 *i*Pr); ^1H NMR (500.3 MHz, $CDCl_3$, 0 °C): $\delta = 7.35$ [(pseudo-t)d, $^3J(H,H) = {}^4J(P,H) = 7.9$ Hz, $^4J(H,H) = 1.5$ Hz, 1H; H_{arom}], 7.32 (ddd, $^3J(H,H) = 7.9$ Hz, $^3J(P,H) = 3.9$ Hz, $^4J(H,H) = 1.5$ Hz, 1H; H_{arom}), 7.26 [(pseudo-t)t, $^3J(H,H) = 7.9$ Hz, $^4J(P,H) = 1.5$ Hz, $^4J(H,H) =$ 1.5 Hz, 1H; H_{arom}], 7.09 [(pseudo-t)t, $^3J(H,H) = 7.9$ Hz, $^4J(P,H) = {}^4J(H,H) = 1.5$ Hz, 1H; H_{arom}], 4.96 (m, 2H; CH_{alkene} nbd), 3.85 (m, 2H; CH nbd), 3.70 (m, 2H; CH_{alkene} nbd), 2.34 (br d, $J(H,H) = 11.7$ Hz, 2H; Cy), 1.91 (sept d, $^2J(P,H) = 7.3$ Hz, $^3J(H,H) = 7.1$ Hz, 2H; CH *i*Pr), 1.80 (br d, $J(H,H) = 12.0$ Hz, 2H; Cy), 1.71 (m, 6H; Cy), 1.49 (m, 1H; CH_2 nbd), 1.44 (m, 1H; CH_2 nbd), 1.34–1.22 (m, 8H; Cy), 1.21 (m, 2H; Cy), 1.20 (dd, $^3J(P,H) = 15.8$ Hz, $^3J(H,H) = 7.1$ Hz, 6H; CH_3 *i*Pr), 1.18 (dd, $^3J(P,H) = 13.1$ Hz, $^3J(H,H) = 7.1$ Hz, 6H; CH_3 *i*Pr), 1.10 ppm (m, 2H; Cy). Elemental analysis calcd (%) for $C_{31}H_{48}BClRhP$: C 61.97, H 8.05; found: C 61.12, H 8.52.

[PdCl(allyl)($PBMes_2$)] **8***:* A suspension of [Pd(μ-Cl)(allyl)]$_2$ (84 mg, 0.23 mmol) in CH_2Cl_2 (3 mL) at room temperature was added to a solution of ligand $PBMes_2$ (200 mg, 0.45 mmol) in CH_2Cl_2 solution (3 mL) at −78 °C. After warming the solution to room temperature within 1 h, the volatiles were removed. Yellow crystals of **8** (121 mg, 42%) suitable for X-ray crystallography were obtained from a Et_2O/THF solution at −40 °C; m.p. 133–135 °C; $^{31}P\{^1H\}$ NMR (202.5 MHz, $CDCl_3$, −20 °C): $\delta =$ 50.8 ppm; ^{11}B NMR (160.5 MHz, $CDCl_3$, 90 °C): $\delta = 73$ ppm; $^{13}C\{^1H\}$ NMR (125.8 MHz, [D_8]THF, −20 °C): $\delta = 144.8$ (br, C_{arom}), 142.6 (d, $J(P,C) = 11.1$ Hz; CH_{arom}), 141.2 (d, $J(P,C) = 3.1$ Hz; C_{arom}), 137.6 (s; C_{arom}), 136.7 (s; C_{arom}), 136.5 (s; C_{arom}), 131.8 (br; CH_{arom}), 130.9 (s; CH_{arom}), 129.9 (s; CH_{arom}), 126.7 (s; CH_{Mes}), 125.6 (s; CH_{Mes}), 115.4 (d, $J(P,C) = 3.5$ Hz; CH_{allyl}), 78.1 (d, $J(P,C) = 30.2$ Hz; CH_{2allyl}), 56.3 (s; CH_{2allyl}), 27.1 (d, $J(P,C) = 3.3$ Hz; CH_{3Mes}), 25.7 (d br, $J(P,C) = 25.7$; CH_{iPr}), 21.7 (s; CH_{3Mes}), 20.5 (s; CH_{3Mes}), 19.8 (s; CH_{3Mes}), 18.1 (s; CH_{3iPr}), 16.6 ppm (s; CH_{3iPr}); ^1H NMR (125.8 MHz, [D_8]THF, −20 °C): $\delta = 7.72$ (pseudo-t, 1H, $^3J(H,H) = J(H,P) = 7.5$ Hz; H_{arom}), 7.68 (m 1H; H_{arom}),

7.54 (pseudo-t, 1H, ^3J(H,H) = 7.5 Hz; H_{arom}), 7.48 (m, 1H; H_{arom}), 6.86 (s, 2H; H_{Mes}), 6.48 (s, 2H; H_{Mes}), 5.41 (tt, 1H, J(H,H) = 6.5 Hz, J(H,H) = 13.0 Hz; H_{allyl}), 4.28 (pseudo-t, 1H, J(H,H) = J(P,H) = 6.5 Hz; H_{allyl}), 3.37 (br d, 1H, J(H,H) = 6.5 Hz; H_{allyl}), 2.73 (m, 2H; CH_{iPr}), 2.62 (s, 6H; CH_{3Mes}), 2.32 (s, 3H; CH_{3Mes}), 2.31 (s, 6H; CH_{3Mes}), 2.17 (s, 3H; CH_{3Mes}), 1.16 (dd, 6H, ^3J(P,H) = 15.0 Hz; CH_{3iPr}), 1.05 ppm (dd, 6H, ^3J(P,H) = 15.0 Hz; CH_{3iPr}).

Crystal Structure Determinations

Data were collected on a Brucker-AXS CCD 1000 diffractometer using an oil-coated shock-cooled crystal. Semiempirical absorption corrections were employed for **5**, **7**, and **8**.[23] The structure was solved by direct methods (SHELXS-97),[24] and refined using the least-squares method on F^2.[25]

Crystal data for **5**: $C_{25.5}H_{43}BCl_5PPd$, M_r = 675.03, monoclinic, space group $P2_1/C$, a = 11.2828(11), b = 15.1977(15), c = 17.8813(18) Å, β = 94.243(2), V = 3057.7(5) Å^3, Z = 4, ρ_{calcd} = 1.466 g cm^{-3}, F(000) = 1388, T = 133(2) K, crystal size 0.01 × 0.1 × 0.1 mm^3, 15317 reflections collected (5162 independent, R_{int} = 0.0972), $2\theta \leq 49.42°$, 316 parameters, $R1$ [$I > 2\sigma(I)$] = 0.0518, $wR2$ [all data] = 0.0848, largest diff. peak and hole: 0.511 and −0.444 e Å^{-3}.

Crystal data for **6**: $C_{42.50}H_{56}BCl_3P_2Pd$, M_r = 852.37, monoclinic, space group $C2/c$, a = 41.141(2), b = 12.3098(7), c = 17.0541(10) Å, β = 104.8740(10)°, V = 8347.4(8) Å^3, Z = 8, ρ_{calcd} = 1.356 g cm^{-3}, F(000) = 3544, T = 133(2 K, crystal size 0.1 × 0.3 × 0.5 mm^3, 24254 reflections collected (8536 independent, R_{int} = 0.0841), $2\theta \leq 52.78°$, 519 parameters, $R1$ [$I > 2\sigma(I)$] = 0.0402, $wR2$ [all data] = 0.0827, largest diff. peak and hole: 0.595 and −0.632 e Å^{-3}.

Crystal data for **7**: $C_{31}H_{48}BClPRh$, M_r = 600.83, monoclinic, space group = $P21/c$, a = 13.0041(7), b = 13.8194(8), c = 16.3131(9) Å, β = 97.7400(10)°, V = 2904.9(3) Å^3, Z = 4, ρ_{calcd} = 1.374 g cm^{-3}, F(000) = 1264, T = 133(2 K, crystal size 0.1 × 0.3 × 0.6 mm^3, 16856 reflections collected (5947 independent, R_{int} = 0.0212), $2\theta \leq 52.78°$, 320 parameters, $R1$ [$I > 2\sigma(I)$] = 0.0227, $wR2$ [all data] = 0.0598, largest diff. peak and hole: 0.429 and −0.469 e Å^{-3}.

Crystal data for **8**: $C_{33}H_{45}BClPPd$, M_r = 625.32, triclinic, space group $P\bar{1}$, a = 9.997(3), b = 10.740(3), c = 14.848(4) Å, α = 78.838(5)°, β = 82.918(4)°, γ = 85.574(5)°, V = 1549.9(7) Å^3, Z = 2, ρ_{calcd} = 1.340 g cm^{-3}, F(000) = 652, T = 133(2 K, crystal size 0.5 × 0.7 × 0.8 mm^3, 9110 reflections collected (6224 independent, R_{int} = 0.0265), $2\theta \leq 53.02°$, 389 parameters, $R1$ [$I > 2\sigma(I)$] = 0.0390, $wR2$ [all data] = 0.0949, largest diff. peak and hole: 0.674 and −0.488 e Å^{-3}.

CCDC 704600, 704601, 704602, and 704603 contain the supplementary crystallographic data for this paper. These data can be obtained free of charge from The Cambridge Crystallographic Data Centre via www.ccdc.cam.ac.uk/data_request/cif.

Computational Details

Calculations were performed with the Gaussian 03 program,[26] using the density functional method. The nonlocal B3PW91[27] functional was used. B3PW91 is Becke's 3 parameter functional, with the nonlocal correlation provided by the Perdew 91 expression. All Gaussian calculations were done in combination with the 6–31G** basis set for C, P, B, Cl, and H (all atoms were augmented with a single set of polarization functions) and the set-RECP (relativistic effective core potential) SDD[28] for Pd and Rh. SDD is the combination of the Huzinaga–Dunning double ζ basis set on lighter elements with the Stuttgart/Dresden basis set-RECP on transition metals. Geometry optimizations were carried out without symmetry restrictions. The optimized structures were confirmed as true minima on the potential energy through vibrational analysis. The frequencies were calculated with analytical second derivatives. All total energies have been zero-point energy (ZPE), and the temperature was corrected using unscaled density functional frequencies. The free Gibbs energies, G, were calculated for T = 298.15 K. The electronic structure of the complexes was studied using natural bond orbital (NBO) analysis.[29] The NBO-3.1 program was used to gain insight into the nature of the interaction between the boron and chloride atoms (bridging form) and to evaluate the energy of the donor/acceptor interaction. ^{11}B NMR chemical shifts were evaluated by employing the direct implementation of the Gauge Including Atomic Orbitals (GIAO) method[30] at the B3PW91 density functional level of theory, using as reference the BF_3-Et_2O compound.

Detailed computational results and cartesian coordinates for the optimized geometries of complexes **3***, **6***, **7***, and **8*** at the B3PW91/SDD(M),6–31G**(other atoms) level of theory are included in the supporting information.

Acknowledgements

We are grateful to the CNRS, UPS, and ANR program (project BILI) for financial support of this work, to the EPSRC solid-state NMR service (Durham) for solid-state NMR spectra, and to M3PEC-Mésocentre (Aquitaine-Bordeaux 1, France) for calculation facilities. Dr. H. Gornitzka is acknowledged for his assistance in the X-ray diffraction analysis of complexes **3** and **7**.

[1] Ambiphilic compounds have also been investigated as multicenter catalysts,[2] molecular sensors,[3] π-conjugated materials,[4] dihydrogen activators,[5] precursors for photoisomerizable heterodienes,[6] and mechanistic probes.[7]

[2] a) G. J. Rowlands, *Tetrahedron* **2001**, *57*, 1865–1882; b) H. Gröger, *Chem. Eur. J.* **2001**, *7*, 5246–5251; c) M. Shibasaki, M. Kanai, K. Funabashi, *Chem. Commun.* **2002**, 1989–1999; d) J.-A. Ma, D. Cahard, *Angew. Chem.* **2004**, *116*, 4666–4683; *Angew. Chem. Int. Ed.* **2004**, *43*, 4566–4583.

[3] a) T. D. James, K. R. A. S. Sandanayake, S. Shinkai, *Angew. Chem.* **1996**, *108*, 2038–2050; *Angew. Chem. Int. Ed. Engl.* **1996**, *35*, 1910–1922; b) L. Zhu, Z. Zhong, E. V. Anslyn, *J. Am. Chem. Soc.* **2005**, *127*, 4260–4269; c) C. Bresner, S. Aldridge, I. A. Fallis, C. Jones, L.-L. Ooi, *Angew. Chem.* **2005**, *117*, 3672–3675; *Angew. Chem. Int. Ed.* **2005**, *44*, 3606–3609.

[4] a) C. D. Entwistle, T. B. Marder, *Angew. Chem.* **2002**, *114*, 3051–3056; *Angew. Chem. Int. Ed.* **2002**, *41*, 2927–2931; b) C. D. Entwistle, T. B. Marder, *Chem. Mater.* **2004**, *16*, 4574–4585; c) T. Agou, J. Kobayashi, T. Kawashima, *Org. Lett.* **2005**, *7*, 4373–4376; d) T. Agou, J. Kobayashi, T. Kawashima, *Chem. Eur. J.* **2007**, *13*, 8051–8060 and references therein.

[5] a) G. C. Welch, R. R. San Juan, J. D. Masuda, D. W. Stephan, *Science* **2006**, *314*, 1124–1126; b) P. A. Chase, G. C. Welch, T. Jurca, D. W. Stephan, *Angew. Chem.* **2007**, *119*, 8196–8199; *Angew. Chem. Int. Ed.* **2007**, *46*, 8050–8053; c) P. Spies, G. Erker, G. Kehr, K. Bergander, R. Fröhlich, S. Grimme, D. W. Stephan, *Chem. Commun.* **2007**, 5072–5074; d) G. C. Welch, L. Cabrera, P. A. Chase, E. Hollink, J. D. Masuda, P. Wei, D. W. Stephan, *Dalton Trans.* **2007**, 3407–3414; e) P. Spies, S. Schwendemann, S. Lange, G. Kehr, R. Fröhlich, G. Erker, *Angew. Chem.* **2008**, *120*, 7654–7657; *Angew. Chem. Int. Ed.* **2008**, *47*, 7543–7546.

[6] M. Bebbington, S. Bontemps, G. Bouhadir, D. Bourissou, *Angew. Chem.* **2007**, *119*, 3397–3400; *Angew. Chem. Int. Ed.* **2007**, *46*, 3333–3336.

[7] S. Moebs-Sanchez, G. Bouhadir, N. Saffon, L. Maron, D. Bourissou, *Chem. Commun.* **2008**, 3435–3437.

[8] The ability of Lewis acids to act as σ-acceptor ligands was recognized early on, and referred to as *Z-type* ligands: a) R. B. King, *Adv. Chem. Ser.* **1967**, *62*, 203–220; b) M. L. H. Green, *J. Organomet. Chem.* **1995**, *500*, 127–148.

[9] Transition metal→borane interactions were first structurally authenticated within metallaboratranes deriving from hydrido tris(imazolyl)borate ligands: a) A. F. Hill, G. R. Owen, A. J. P. White, D. J. Williams, *Angew. Chem.* **1999**, *111*, 2920–2923; *Angew. Chem. Int. Ed.* **1999**, *38*, 2759–2761; b) M. R. St.-J. Foreman, A. F. Hill, A. J. P. White, D. J. Williams, *Organometallics* **2004**, *23*, 913–916; c) D. J. Mihalcik, J. L. White, J. M. Tanski, L. N. Zakharov, G. P. A. Yap, C. D. Incarvito, A. L. Rheingold, D. Rabinovitch, *Dalton Trans.*

2004, 1626–1634; d) I. R. Crossley, A. F. Hill, A. C. Willis, *Organometallics* **2005**, *24*, 1062–1064; e) I. R. Crossley, A. F. Hill, E. R. Humphrey, A. C. Willis, *Organometallics* **2005**, *24*, 4083–4086; f) I. R. Crossley, M. R. St.-J. Foreman, A. F. Hill, A. J. P. White, D. J. Williams, *Chem. Commun.* **2005**, 221–223; g) I. R. Crossley, A. F. Hill, A. C. Willis, *Organometallics* **2006**, *25*, 289–299; h) V. K. Landry, J. G. Melnick, D. Buccella, K. Pang, J. C. Ulichny, G. Parkin, *Inorg. Chem.* **2006**, *45*, 2588–2597; i) S. Senda, Y. Ohki, T. Hirayama, D. Toda, J.-L. Chen, T. Matsumoto, H. Kawaguchi, K. Tatsumi, *Inorg. Chem.* **2006**, *45*, 9914–9925; j) K. Pang, S. M. Quan, G. Parkin, *Chem. Commun.* **2006**, 5015–5017; k) J. S. Figueroa, J. G. Melnick, G. Parkin, *Inorg. Chem.* **2006**, *45*, 7056–7058; l) R. J. Blagg, J. P. H. Charmant, N. G. Connelly, M. F. Haddow, A. G. Orpen, *Chem. Commun.* **2006**, 2350–2352; m) I. R. Crossley, A. F. Hill, A. C. Willis, *Organometallics* **2008**, *27*, 312–315; n) I. R. Crossley, M. R. St.-J. Foreman, A. F. Hill, G. R. Owen, A. J. P. White, D. J. Williams, A. C. Willis, *Organometallics* **2008**, *27*, 381–386; o) K. Pang, J. M. Tanski, G. Parkin, *Chem. Commun.* **2008**, 1008–1010.

[10] a) S. Bontemps, H. Gornitzka, G. Bouhadir, K. Miqueu, D. Bourissou, *Angew. Chem.* **2006**, *118*, 1641–1644; *Angew. Chem. Int. Ed.* **2006**, *45*, 1611–1614; b) S. Bontemps, G. Bouhadir, K. Miqueu, D. Bourissou, *J. Am. Chem. Soc.* **2006**, *128*, 12056–12057; c) S. R. Oakley, K. D. Parker, D. J. H. Emslie, I. Vargas-Baca, C. M. Robertson, L. E. Harrington, J. F. Britten, *Organometallics* **2006**, *25*, 5835–5838; d) M. Sircoglou, S. Bontemps, M. Mercy, N. Saffon, M. Takahashi, G. Bouhadir, L. Maron, D. Bourissou, *Angew. Chem.* **2007**, *119*, 8737–8740; *Angew. Chem. Int. Ed.* **2007**, *46*, 8583–8586; e) S. Bontemps, M. Sircoglou, G. Bouhadir, H. Puschmann, J. A. K. Howard, P. W. Dyer, K. Miqueu, D. Bourissou, *Chem. Eur. J.* **2008**, *14*, 731–740; f) S. Bontemps, G. Bouhadir, W. Gu, M. Mercy, C.-H. Chen, B. M. Foxman, L. Maron, O. V. Ozerov, D. Bourissou, *Angew. Chem.* **2008**, *120*, 1503–1506; *Angew. Chem. Int. Ed.* **2008**, *47*, 1481–1484; g) D. J. H. Emslie, L. E. Harrington, H. A. Jenkins, C. M. Robertson, J. F. Britten, *Organometallics* **2008**, *27*, 5317–5325; h) M. Sircoglou, S. Bontemps, G. Bouhadir, N. Saffon, K. Miqueu, W. Gu, M. Mercy, C.-H. Chen, B. M. Foxman, L. Maron, O. V. Ozerov, D. Bourissou, *J. Am. Chem. Soc.* **2008**, *130*, 16729–16738; i) F.-G. Fontaine, J. Boudreau, M.-H. Thibault, *Eur. J. Inorg. Chem.* **2008**, 5439–5454; j) I. Kuzu, I. Krummenacher, J. Meyer, F. Armbruster, F. Breher, *Dalton Trans.* **2008**, 5836–5865.

[11] a) A. Börner, J. Ward, K. Kortus, H. B. Kagan, *Tetrahedron: Asymmetry* **1993**, *4*, 2219–2228; b) L. B. Fields, E. N. Jacobsen, *Tetrahedron: Asymmetry* **1993**, *4*, 2229–2240; c) H. Braunschweig, R. Dirk, B. Ganter, *J. Organomet. Chem.* **1997**, *545–546*, 257–266; d) D. J. H. Emslie, J. M. Blackwell, J. F. Britten, L. E. Harrington, *Organometallics* **2006**, *25*, 2412–2414; e) J. Vergnaud, M. Grellier, G. Bouhadir, L. Vendier, S. Sabo-Etienne, D. Bourissou, *Organometallics* **2008**, *27*, 1140–1146; f) S. Chikkali, S. Magens, D. Gudat, M. Nieger, I. Hartenbach, T. Schleid, *Eur. J. Inorg. Chem.* **2008**, 2207–2213; g) A. J. M. Miller, J. A. Labinger, J. E. Bercaw, *J. Am. Chem. Soc.* **2008**, *130*, 11874–11875.

[12] a) R. T. Baker, J. C. Calabrese, S. A. Westcott, T. B. Marder, *J. Am. Chem. Soc.* **1995**, *117*, 8777–8784; b) S. J. Lancaster, S. Al-Benna, M. Thornton-Pett, M. Bochmann, *Organometallics* **2000**, *19*, 1599–1608; c) T. J. Crevier, B. K. Bennett, J. D. Soper, J. A. Bowman, A. Dehestani, D. A. Hrovat, S. Lovell, W. Kaminsky, J. M. Mayer, *J. Am. Chem. Soc.* **2001**, *123*, 1059–1071; d) J. Vergnaud, T. Ayed, K. Hussein, L. Vendier, M. Grellier, G. Bouhadir, J.-C. Barthelat, S. Sabo-Etienne, D. Bourissou, *Dalton Trans.* **2007**, 2370–2372.

[13] a) F.-G. Fontaine, D. Zargarian, *J. Am. Chem. Soc.* **2004**, *126*, 8786–8794; b) M.-H. Thibault, J. Boudreau, S. Mathiotte, F. Drouin, O. Sigouin, A. Michaud, F.-G. Fontaine, *Organometallics* **2007**, *26*, 3807–3815.

[14] a) A. Fischbach, P. R. Bazinet, R. Waterman, T. D. Tilley, *Organometallics* **2008**, *27*, 1135–1139; b) M. Sircoglou, G. Bouhadir, N. Saffon, K. Miqueu, D. Bourissou, *Organometallics* **2008**, *27*, 1675–1678.

[15] G. Aullón, G. Ujaque, A. Lledós, S. Alvarez, P. Alemany, *Inorg. Chem.* **1998**, *37*, 804–813.

[16] Similarly, (4-dimethylamino)pyridine DMAP was found to selectively react with the dinuclear complex $[Rh(\mu\text{-}Cl)(DPB)]_2$ {DPB = [*o*-$iPr_2P(C_6H_4)]_2BPh$} with cleavage of the chloro bridge rather than that of the Rh→B interaction.[10a]

[17] See for example: a) F. B. Ogilvie, J. M. Jenkins, J. G. Verkade, *J. Am. Chem. Soc.* **1970**, *92*, 1916–1923; b) R. J. Goodfellow, B. F. Taylor, *J. Chem. Soc. Dalton Trans.* **1974**, 1676–1684.

[18] S. Bontemps, G. Bouhadir, P. W. Dyer, K. Miqueu, D. Bourissou, *Inorg. Chem.* **2007**, *46*, 5149–5151.

[19] Such an equilibrium between the bridging and B-pendant forms may explain that no distinct ^{11}B NMR signal could be detected for **5** and **6** in solution.

[20] a) D. V. Partyka, T. J. Robilotto, M. Zeller, A. D. Hunter, T. G. Gray, *Organometallics* **2008**, *27*, 28–32; b) D. V. Partyka, M. P. Washington, J. B. Updegraff III, R. A. Woloszynek, J. D. Protasiewicz, *Angew. Chem.* **2008**, *120*, 7599–7602; *Angew. Chem. Int. Ed.* **2008**, *47*, 7489–7492.

[21] Although aryl dimesitylboranes normally only bind fluoride, the geometric constraint induced by the rigid $R_2P\text{-}o(C_6H_4)BMes_2$ skeleton was recently found to allow the interaction of the $BMes_2$ group with larger Lewis bases.[6,7]

[22] The coexistence of the bridging and B-pendant forms suggests some hemilabile character for the ambiphilic $PBCy_2$ ligand. For a recent review on the hemilability of hybrid ligands, see: P. Braunstein, F. Naud, *Angew. Chem.* **2001**, *113*, 702–722; *Angew. Chem. Int. Ed.* **2001**, *40*, 680–699.

[23] SADABS, Program for data correction, Bruker-AXS.

[24] G. M. Sheldrick, *Acta Crystallogr. Sect. A* **1990**, *46*, 467–473.

[25] SHELXL-97, Program for Crystal Structure Refinement, G. M. Sheldrick, University of Göttingen, **1997**.

[26] *Gaussian 03*, Revision B.05, M. J. Frisch, G. W. Trucks, H. B. Schlegel, G. E. Scuseria, M. A. Robb, J. R. Cheeseman, J. A. Montgomery, Jr. T. Vreven, K. N. Kudin, J. C. Burant, J. M. Millam, S. S. Iyengar, J. Tomasi, V. Barone, B. Mennucci, M. Cossi, G. Scalmani, N. Rega, G. A. Petersson, H. Nakatsuji, M. Hada, M. Ehara, K. Toyota, R. Fukuda, J. Hasegawa, M. Ishida, T. Nakajima, Y. Honda, O. Kitao, H. Nakai, M. X. Klene, X. Li, J. E. Knox, H. P. Hratchian, J. B. Cross, C. Adamo, J. Jaramillo, R. Gomperts, R. E. Stratmann, O. Yazyev, A. J. Austin, R. Cammi, C. Pomelli, J. W. Ochterski, P. Y. Ayala, K. Morokuma, G. A. Voth, P. Salvador, J. J. Dannenberg, V. G. Zakrzewski, S. Dapprich, A. D. Daniels, M. C. Strain, O. Farkas, D. K. Malick, A. D. Rabuck, K. Raghavachari, J. B. Foresman, J. V. Ortiz, Q. Cui, A. G. Baboul, S. Clifford, J. Cioslowski, B. B. Stefanov, G. Liu, A. Liashenko, P. Piskorz, I. Komaromi, R. L. Martin, D. J. Fox, T. Keith, M. A. Al-Laham, C. Y. Peng, A. Nanayakkara, M. Challacombe, P. M. W. Gill, B. Johnson, W. Chen, M. W. Wong, C. Gonzalez, J. A. Pople, Gaussian, Inc., Pittsburgh PA, **2003**.

[27] a) A. D. Becke, *Phys. Rev. A* **1988**, *38*, 3098–3100; b) J. P. Perdew, *Phys. Rev. B* **1986**, *33*, 8822–8824; Erratum: c) J. P. Perdew, *Phys. Rev. B* **1986**, *34*, 7406; d) A. D. Becke, *J. Chem. Phys.* **1993**, *98*, 5648–5652; e) K. Burke, J. P. Perdew, Y. Wang, *Electronic Density Functional Theory: Recent Progress and New Directions* (Eds.: J. F. Dobson, G. Vignale, M. P. Das), Plenum, New York, **1998**.

[28] a) M. Dolg, *Modern Methods and Algorithm of Quantum Chemistry, Vol. 1* (Ed.: J. Grotendorst), John von Neuman Institute for Computing, Jülich, Germany, **2000**, pp. 479–508; b) M. Dolg, U. Wedig, H. Stoll, H. Preuss, *J. Chem. Phys.* **1987**, *86*, 866–872; c) D. Andrae, U. Häussermann, M. Dolg, H. Stoll, H. Preuss, *Theor. Chim. Acta.* **1990**, *77*, 123–141.

[29] a) A. E. Reed, L. A. Curtiss, F. Weinhold, *Chem. Rev.* **1988**, *88*, 899–926; b) J. P. Foster, F. Weinhold, *J. Am. Chem. Soc.* **1980**, *102*, 7211–7218.

[30] a) F. London, *J. Phys. Radium* **1937**, *8*, 3974–3976; b) R. Ditchfield, *Mol. Phys.* **1974**, *27*, 789–807; c) K. Wolinski, J. F. Hilton, P. Pulay, *J. Am. Chem. Soc.* **1990**, *112*, 8251–8260.

Received: October 9, 2008
Published online: January 7, 2009

